



ELSEVIER

JOURNAL OF
PHYSICS AND CHEMISTRY
OF SOLIDS

Journal of Physics and Chemistry of Solids 61 (2000) 1553–1560

www.elsevier.nl/locate/jpcs

Effect of Pb addition on thermoelectric power and microhardness of Bi–Pb–Sr–Ca–Cu–O superconductors

M.M. Ibrahim, S.M. Khalil*, A.M. Ahmed

Physics Department, Faculty of Science, South Valley University, Sohag, Egypt

Received 8 December 1999; accepted 22 February 2000

Abstract

The effect of (Pb) addition on the zero thermopower temperature (T_c^0) and room temperature Vickers microhardness (VHN) of superconducting specimens of different nominal compositions based on the system $\text{Bi}_{2-x}\text{Pb}_x\text{Sr}_2\text{Ca}_2\text{Cu}_3\text{O}_y$ ($x = 0.0, 0.1, 0.2, 0.3$ and 0.5) were studied. The addition of (0.3Pb) resulted in an increase in T_c^0 from 93 to 113 K and a 2.85-fold increase in the microhardness for considered loads. This behaviour is ascribed to the presence of large amount of the high- T_c phase (2223). Furthermore, Pb particles may relax the residual stresses resulting from the expansion of individual grains, and may provide increased resistance to crack propagation by pinning the propagating cracks; these effects would increase the hardness. The addition of (0.5Pb) resulted in a decrease in T_c^0 to 98 K, and also VHN decreases almost 2.44 times. This decrease in T_c^0 and VHN is believed to be due to the formation of contaminating phases such as Ca_2PbO_4 . Indexed X-ray diffraction patterns indicated that high abundance of the 2223 phase for the specimen (0.3Pb) are characterized by the sharpest superconducting transitions. Also the present study proved that the most convenient Pb content to obtain a minimum value of porosity is equal (0.3Pb). © 2000 Elsevier Science Ltd. All rights reserved.

Keywords: A. Oxides; D. Mechanical properties; D. Superconductivity

1. Introduction

After the discovery of high- T_c superconducting in the Bi–Sr–Ca–Cu–O system by Meda et al. [1], Tallon et al. [2] reported that Bi-compounds (BSCCO) posses three superconducting transitions viz. at 110 K (2223 phase), 80 K (2212 phase) and 10 K (2201 phase). Normal state properties of the high T_c superconductors have attracted significant research interest. This is due to the fact that many of these compounds show unusual normal state properties and the expectation that a proper understanding of their properties in the normal state may provide clues to the origin of superconductivity in this class of materials. Among many other normal state properties, thermoelectric power sensitivity depends on the energy dependence of the electron lifetime and the density of states near the Fermi energy (E_F). Therefore, studies on the temperature dependence of thermoelectric power can provide excellent information about many fundamental aspects of charge transport in ceramic super-

conductors. Besides the usual resistance measurements to determine the resistive superconducting transition temperature in $\text{Sb}-\text{BiPbSrCaCuO}_y$ investigated by Kocabas [3].

Normal state thermoelectric power (TEP) of ceramic superconductors have been reported by Sergeevkov et al. [4]. Also more consistency in the reported data has been observed for the TEP of the Bi-based and TL-based cuprate superconductors [5,6]. Thermoelectric power in these systems is usually a few $\mu\text{V/K}$, typical of a metal with low carrier density. Its sign is commonly positive, which is consistent with the charge carrier sign measured by the Hall effect, though the sign of TEP has been found to be sometimes negative [7,8]. Attention is focused on lead containing compounds of the general formula $\text{Pb}_x\text{Bi}_{2-x}\text{Sr}_2\text{Ca}_2\text{Cu}_3\text{O}_y$ [9].

On the other hand, there is another important factor for the practical usage of oxide superconductors. For most applications, these materials have to be drawn in the form of wires and tapes. These superconducting wires and tapes are subjected to large mechanical stresses in making coils and Lorentz force due to high magnetic fields. Under high

* Corresponding author. Fax: +93601950/159.

E-mail address: janoubwadi@frcu.eun.eg (S.M. Khalil).

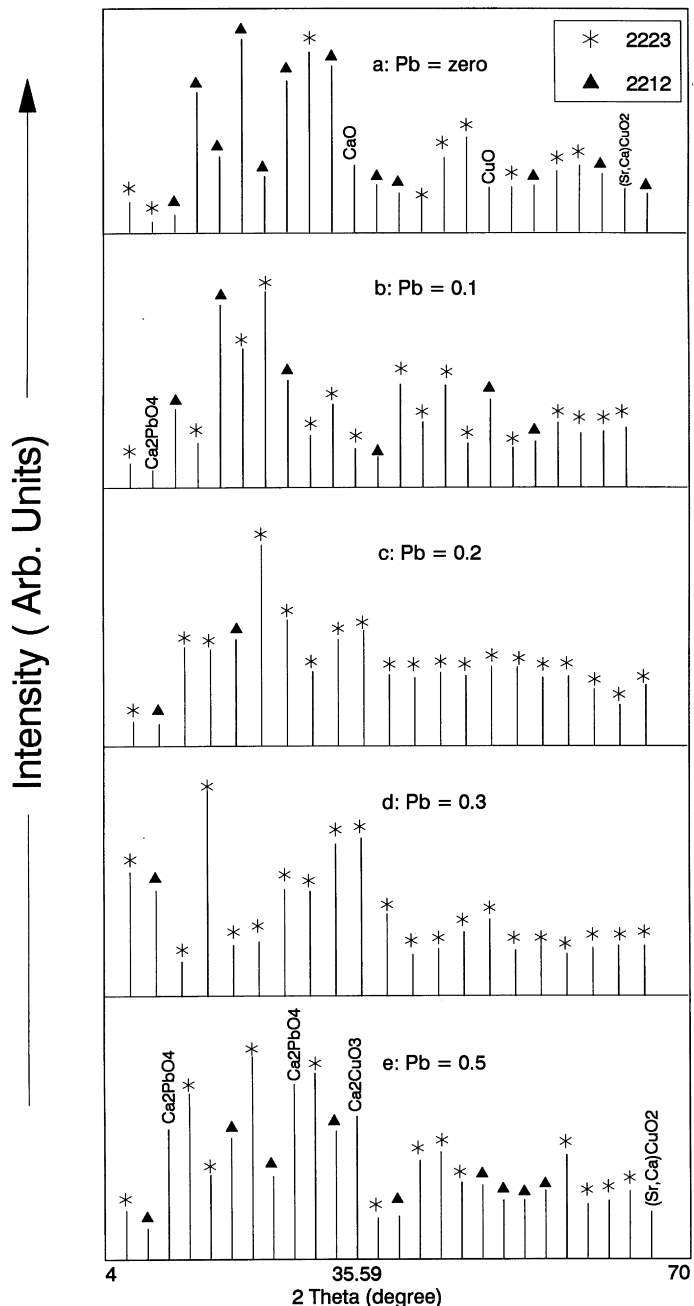


Fig. 1. Typical powder X-ray diffraction patterns of $\text{Bi}_{2-x}\text{Pb}_x\text{Sr}_2\text{Ca}_2\text{Cu}_3\text{O}_y$ with lead concentration.

stresses, the generation of small cracks at high current will cause a fatal damage or destruction of the coil. Therefore, the evaluation of mechanical properties of superconductors is important for their practical applications. Flexural strength [10], tensile strength [11,12], microhardness [13–16], and elastic modules [17–19] have been reported for Y–Ba–Cu–O compounds. Besides this, there are few works on the mechanical properties of Bi-based (BSCCO) supercon-

ductors. Goto has reported a tensile strength of 55 MPa for the $\text{Bi}_2\text{Sr}_2\text{Ca}_2\text{Cu}_3\text{O}_x$ (2223) fibre prepared by Suspension Spinning method [20]. Johnson et al. [21] have reported on a relationship between the bulk density and the bending strength of $\text{Bi}_2\text{Sr}_2\text{CaCu}_2\text{O}_x$ (2212) sintered bodies. They have obtained the maximum value of 32 MPa when the sintering temperature is 910°C. Shoyama et al. [22] have measured the tensile strength of the 2223 fibre prepared

by the pyrolysis of organic acid salts and reported to be 18 MPa. Investigating the effect of lead on the microhardness of the BSCCO system was studied by authors [23,24]. All these data are obtained for polycrystalline compounds, so that grain boundaries, pores, and probably micro cracks in the specimens could predominate these hardness values. The investigation by Verrender et al. [25], explores basic aspects of the route to better materials, paying particular attention to porosity and to the use that can be made of microhardness as a means for assessing the mechanical state of specimens.

In the present article, we report our results on the temperature dependence of TEP of sintered superconducting specimens of different compositions of the system $\text{Bi}_{2-x}\text{Pb}_x\text{Sr}_2\text{Ca}_2\text{Cu}_3\text{O}_y$. Besides this the influence of lead addition on the microhardness of the same specimens was investigated. Also, measurements on porosity percentage were performed and X-ray powder diffraction (XRD) patterns were taken to identify the main phases. Photographs of surfaces were taken using a scanning electron microscope (SEM).

2. Experiments

Superconducting specimens of the five nominal compositions based on the system $\text{Bi}_{2-x}\text{Pb}_x\text{Sr}_2\text{Ca}_2\text{Cu}_3\text{O}_y$, with $x = 0.0, 0.1, 0.2, 0.3$ and 0.5 were prepared by using the solid-state reaction traditional sintering technique. The appropriate amounts of Bi_2O_3 , PbO , SrO , CaCO_3 and CuO powders (with purity equal to 99.999%) were weighed and mixed together in molar ratios as required. The mixtures were dissolved in equivalent amount of conc. HNO_3 . The solution was stirred and heated at 600°C (about 6 h), it becomes dry to form a precipitate with a deep blue colour. The dry precipitate product was then calcined at 820°C in air for 48 h. The product powder was reground and pressed into pellets by applying a load of 49 kN. Pellets were sintered at 845°C for 150 h in air and slowly cooled to room temperature.

The differential thermoelectric power S (Seebeck coefficient) of a sample was measured using the standard differential technique. A specimen was sandwiched between two copper blocks. The lower block contains an independent heater. Thermoelectric voltages were measured relative to the copper leads and in the presence of a temperature gradient (ΔT) about 2–3 K across the specimen. Measurements of the temperature difference between the working surfaces of the specimen under test (ΔT) were done with a differential copper–constantan thermocouple. The data presented here have been corrected for the contribution of copper leads to the measured thermoelectric power.

Diamond pyramid hardness measurements were performed with a type E.Ltd. Wetzlar microhardness tester at room temperature. A Vickers pyramidal indentor, with different loads (0.25, 0.49 and 0.98 N) and a loading time of 15 s was used. A measuring objective was used to

measure the diagonals of the indentation with an accuracy of $\pm 0.5 \mu\text{m}$. An average of 10 readings at different locations of specimen's surface was taken for each specimen.

The Vickers hardness was calculated using the following formula:

$$\text{VHN} = 1.8544(P/d^2)$$

where P is the applied load (in N) and d is the mean length of the diagonal of indentor impression (in mm).

The hardness test requires that the surfaces of a specimen must be highly polished and the specimen should, prior to the hardness test, by focusing the 40:1 objective of the microscope sharply on the surface of the specimen and pressing lightly on it in the immediate vicinity of the objective with a small stick, while observing the surface through the microscope. On the other hand, it is in any case essential to avoid placing the specimen under tension, as this results in curvature any way. Besides, the percentage of the porosity of samples was measured by the Archimedes method using xylene as the immersion liquid.

The XRD analysis was performed by means of a Schemdzu X-ray powder diffractometer with $\text{CuK}\alpha$ target. On the other hand, the surface morphology of the tested specimens was investigated using a SEM type Jeol JSM-5300. A specimen to be tested for its surface morphology has to be highly polished and with a clean surface.

3. Results and discussion

3.1. XRD analysis

In order to clarify the effect of Pb addition, we changed the amount of Pb addition from 0.0 to 0.5 and thoroughly examined the changes by the X-ray diffraction $\text{CuK}\alpha$ radiation. The X-ray diffractograms of samples with $0.0 \leq x \leq 0.5$ are shown in Fig. 1(a)–(e). The appearance of different peaks with different intensities on each of the diffractogram proves beyond doubt either the high- T_c phase (2223) or the low- T_c phase (2212). For the Pb free composition as shown in Fig. 1(a), the most, the third and the fourth intense peaks were the same and could be identified as the 2212 phase, while the second intense peak could be identified as the 2223 phase. Also, some intense peaks due to double oxides such as CuO and CaO were present. This indicates that the low- T_c phase (2212) is dominant in sample (Pb = 0.0).

As shown in Fig. 1(b)–(d) with an increase in the lead content, the number of peaks attributed to the high- T_c phase preferentially grows at the expense of the number of peaks of the low- T_c phase and becomes significant around $x = 0.3$. This implies that the optimized sample (Pb = 0.3) is most convenient for the formation of the high- T_c phase. On the other hand, the absence of other Pb-related peaks such as (PbO , SrPbO_3 , etc.) suggests that the Pb atom is mainly involved in the Bi–Sr–Ca–Cu–O structure. After that for ($x = 0.5$) the number of peaks attributed to the 2223 phase

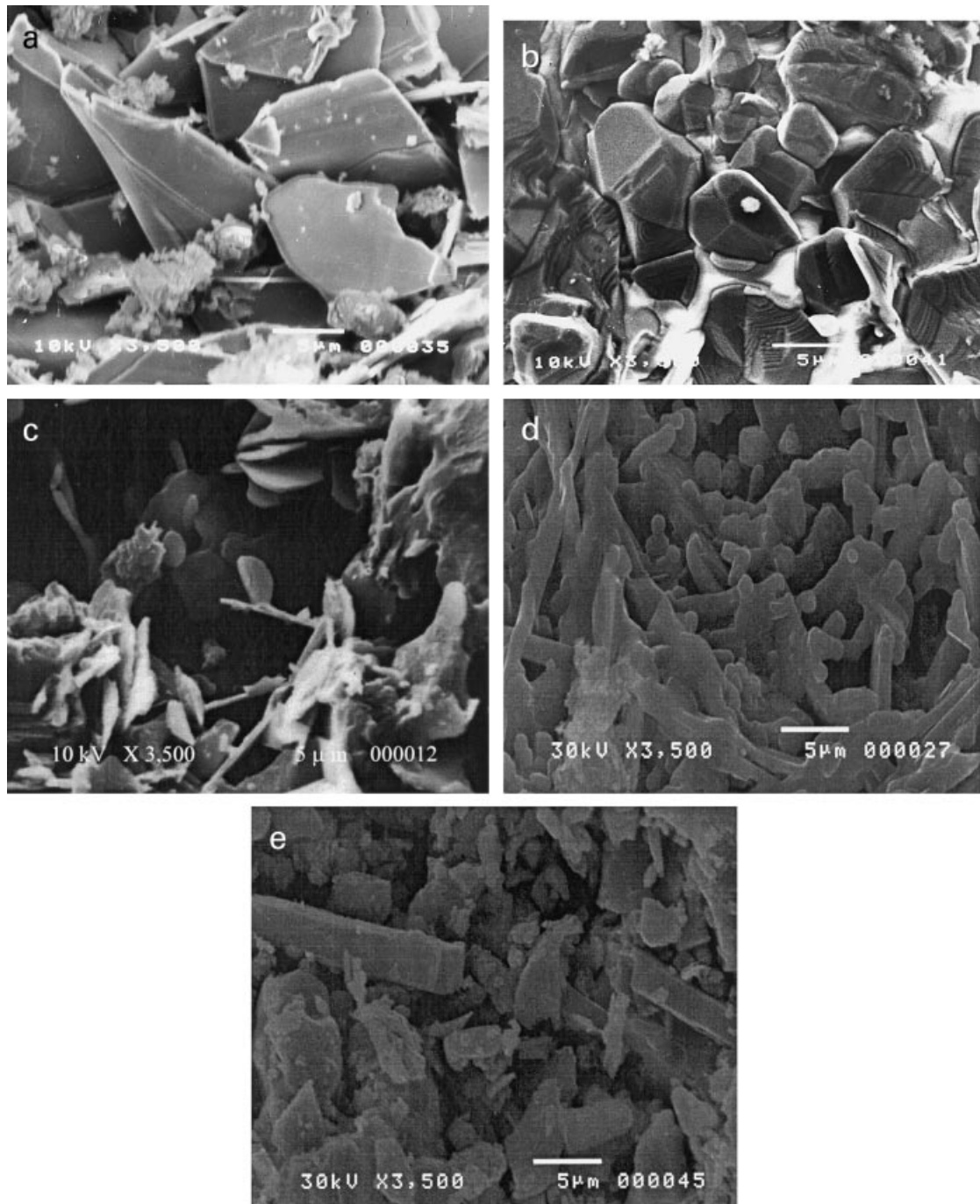


Fig. 2. Photograph showing the morphology of polished surface of the sample (a) $\text{Bi}_2\text{Sr}_2\text{Ca}_2\text{Cu}_3\text{O}_y$; (b) $\text{Bi}_{1.9}\text{Pb}_{0.1}\text{Sr}_2\text{Ca}_2\text{Cu}_3\text{O}_y$; (c) $\text{Bi}_{1.8}\text{Pb}_{0.2}\text{Sr}_2\text{Ca}_2\text{Cu}_3\text{O}_y$; (d) $\text{Bi}_{1.7}\text{Pb}_{0.3}\text{Sr}_2\text{Ca}_2\text{Cu}_3\text{O}_y$; and (e) $\text{Bi}_{1.5}\text{Pb}_{0.5}\text{Sr}_2\text{Ca}_2\text{Cu}_3\text{O}_y$.

are reduced with an increase in the number of peaks of the 2212 phase besides the presence of number of peaks belonging to Ca_2PbO_4 and Ca_2CuO_3 . Mangapathi et al. [26] and Murlidhar et al. [27] also noticed a similar behaviour in the samples fabricated by the ceramic technique. This reduction

in the number of peaks of the 2223 phase may be the consequence of its dissociation into impure phases like Ca_2PbO_4 and Ca_2CuO_3 [28]. However, from these observations of the XRD analysis, we can be sure that the high- T_c phase (2223) is the chief constituent in the sample of $x = 0.3$.

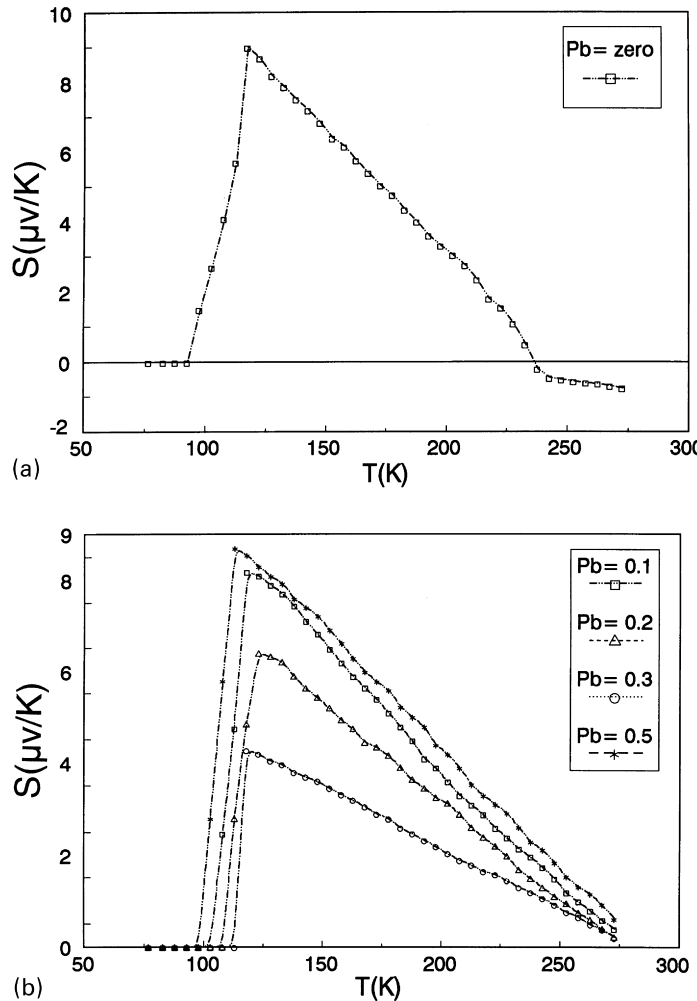


Fig. 3. The variation of TEP with temperature for: (a) $\text{Pb} = 0.0$; and (b) $\text{Pb} = 0.1, 0.2, 0.3$ and 0.5 .

3.2. Scanning electron microscopy

Fig. 2(a)–(c) shows SEM images of polished sections of specimens ($x = 0.0\text{--}0.5$), respectively. As shown in Fig. 2(a) for the Pb free sample, plate-like grains were observed, which were described as a sequence of the 2212 and 2223 layers [29]. These plate-like grains are piled up in random directions and connected weakly to each other. Also, visible particles are formed with low abundance. Based on previous data reported elsewhere [30–32], these visible particles can represent admixed phases such as CaO and CuO which could be identified by XRD analysis. It is obvious from Fig. 2(b) which shows the micrograph corresponding to the sample of 0.1Pb , that there is an increment in the number and a certain degree of preferred orientation and connection of the plate-like grains. Meanwhile, the needle-like grains are observed clearly with an anisotropic orientation in the sample of 0.2 in Fig. 2(c). These grains are considered to

be responsible for the high- T_c phase [28,33–36]. With the enriching of the Pb content ($x = 0.3$), the amount of needle-like grains seems high, well oriented and better connected than the former composition. This remarkable growth of needle-like grains in sample ($\text{Pb} = 0.3$), is responsible for the pore elimination and consequently the increment of T_c^o and VHN of this sample. A lead rich sample ($\text{Pb} = 0.5$) is associated with a decrease in the needle-like grains. Also, the grains are disconnected as a result the presence of minor phases such as Ca_2PbO_4 and $(\text{Sr},\text{Ca})\text{CuO}_2$. It is worth mentioning that columnar grains were also observed. From the analytical results of the energy dispersive X-ray (EDX) it is shown that the columnar grains consisted of Sr, Ca and Cu compounds [37].

Based on the above findings, it concluded that the amount of (0.3Pb) is most convenient for the formation of the high- T_c phase (needle-like grains) while excessive of Pb addition ($x = 0.5$) causes the appearance of the Ca_2PbO_4 phase which

Table 1

Variation of T_c^0 with lead content

| No. | Pb% | T_c^0 (K) |
|-----|-----|-------------|
| 1 | 0.0 | 93 |
| 2 | 0.1 | 103 |
| 3 | 0.2 | 108 |
| 4 | 0.3 | 113 |
| 5 | 0.5 | 98 |

seems to assist the formation of the low- T_c phase in place of the high- T_c phase.

3.3. Thermoelectric power

The temperature dependence of thermoelectric power (S) for the present set of samples ($x = 0.0$ to 0.5) are shown in Fig. 3(a) and (b). For the free lead sample ($x = 0.0$) in Fig. 3(a), the relatively high temperature range of T around 238 K is characterized by a negative sign S ; below this temperature the sign of S reversed to plus and the value of the plus sign S increases linearly with decreasing temperature and has a peak at 118 K. The temperature at which the maximum plus sign S (peak) is reached is denoted as T^{ons} , and depends on the lead content. Below T^{ons} the plus sign S decreases continuously and goes down to zero at temperature about (93 K), this temperature denoted as T_c^0 depends on the lead content and data are tabulated in Table 1. The occurrence of the S peak at temperature well above T_c^0 seems to be the common feature of the high T_c superconductors as has been observed by Canda et al. [38]. The peak is a consequence of a rising phonon drag component turned around due to pair fluctuation effects above T_c [7] and a

transition to the superconducting state where the S has to drop down to zero. However, this result broadly agrees with the data of Forro et al. [39]. Quite a different temperature dependence of S could be observed in Fig. 3(b), for lowest Pb content samples ($x = 0.1$ and 0.2) as shown, thermopower sign is positive over the entire measured temperature range, which nevertheless differs with that for the sample of ($x = 0.0$). Further, its magnitude increases almost linearly upon cooling which is a behaviour typical of semiconductors. As the temperature is lowered to about $T^{ons} \approx 118$ and 123 K, below which S drops down to zero at $T_c^0 \approx 103$ and 108 K, respectively. In fact, the temperature variation of S for these samples is similar to the heavily Sr doped $\text{La}_{1.75}\text{Sr}_{0.25}\text{CuO}_4$ sample of Uher et al.[40]. This has been explained by them in terms of a two bond model with a strong carrier–phonon interaction and a low carrier density. On the other side, the S behaviour of our specimens is very similar to that reported by Jha et al. [7]. They believed that the S variation with temperature can as well be accounted for by assuming electrons and holes as carriers and their strong interaction with phonons. In a system where both electrons and holes are the carriers the electrons' contribution to S dominates because of a strong energy dependence of their mobility. For the medium lead content in sample ($x = 0.3$), S exhibits a relatively small maximum around 118 K, just above the transition temperature. We believe that the small value of S (300) is perhaps due to the presence of a large amount of the high- T_c phase (2223) within the detection limit of the XRD. Below 118 K, a transition to the superconducting state occurs in a very narrow interval at 113 K. It proves the homogeneity of the sample confirmed by the XRD. For a lead rich sample ($x = 0.5$), the S – T dependence was similar in feature to that for $x = 0.3$ but with lower $T^{ons} \sim 113$ K and T_c^0 for compensation was also

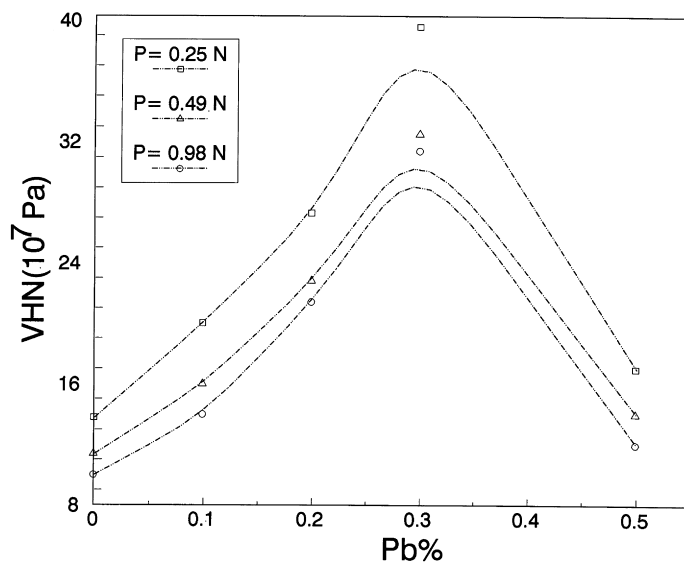


Fig. 4. The variation of microhardness with lead concentration for $\text{Bi}_{2-x}\text{Pb}_x\text{Sr}_2\text{Ca}_2\text{Cu}_3\text{O}_y$. The time of each indentation is 15 s.

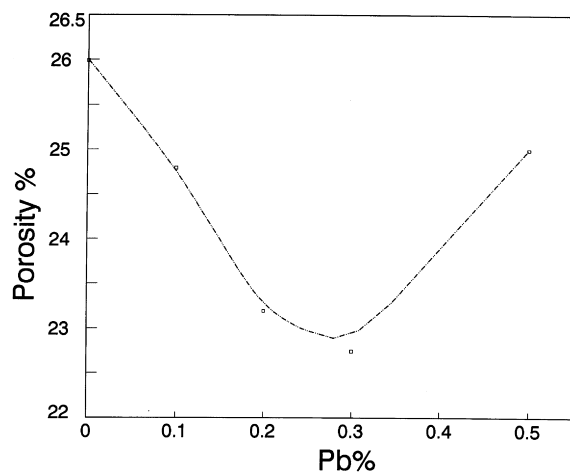


Fig. 5. The variation of porosity with lead concentration for $\text{Bi}_{2-x}\text{Pb}_x\text{Sr}_2\text{Ca}_2\text{Cu}_3\text{O}_y$.

lower about 98 K. A close look at this figure reveals that the lead content involves a remarkable evolution of the temperature variation of S and its T_c^0 . Generally, an increasing lead content up to $\text{Pb} = 0.3$ decreases the plus sign values of S and increases its T_c^0 which may reflect an enriching of the high- T_c phase (2223) with its highest transition temperature on the expense of other existing phases, i.e. in the samples a matter could be emphasized by the XRD analysis. More excess of Pb ($x = 0.5$) is associated with a decrease of T_c^0 and an increase of the plus sign value of S ; this behaviour may be due to the dissociation of the 2223 phase into impure phases like Ca_2PbO_4 and Ca_2CuO_3 . However, the obtained results agree well with those presented in Refs. [7,9,28,34].

3.4. Microhardness measurements

The room temperature Vickers microhardness is plotted as a function of the Pb concentration at three loads (0.25, 0.49 and 0.98 N) as shown in Fig. 4. The microhardness increased monotonically with lead addition up to 0.3, after that it decreased drastically. The addition of 0.3Pb resulted in an increase of microhardness from 11.4×10^7 to 32.5×10^7 Pa at $P = 0.49$ N. Near-linear rise of VHN with (x) is probably caused by solid-solution hardening, while the reduction of VHN with excess of Pb (0.5), may be due to the reduction in the packing forces between superconducting grains. In fact, the 2.85 increase in microhardness, which is attributed to Pb addition (0.3), may relax residual stresses resulting from the expansion of grains and provide an increased resistance to crack propagation by pinning the propagating crack, and thus increase the microhardness. On the other hand, the microhardness decreases almost 4.22 times with increasing Pb content from 0.3 to 0.5. This degradation of VHN owing to the extension crack

induced failure in the grain boundaries would further decrease the measured hardness values.

In the view of this observation, we can be sure that the addition of Pb (up to 0.3) content to the $\text{Bi}-\text{Sr}-\text{Ca}-\text{Cu}-\text{O}$ system stabilizes the high- T_c phase (2223) and therefore hardens the $\text{Bi}_{2-x}\text{Pb}_x\text{Sr}_2\text{Ca}_2\text{Cu}_3\text{O}_y$ ceramics. More excess of Pb(0.5), decreases the bond strength between superconducting grains as a result of the formation of impure phases, consequently the measured values of hardness are decreased. However, this result agrees well with Veerender et al. [25].

Fig. 5 shows the variation of porosity with lead content ($x = 0.0-0.5$) of samples. It can be observed that the porosity decreases with the increase in the lead content until $x = 0.3$ and after that it increases, i.e. the porosity is minimum in that compound which has maximum VHN, smallest positive sign S , sharpest T_c^0 and consisted predominantly of the high- T_c phase (2223). This result implies that the porosity is squeezed by the increase of the Pb content up to 0.3, this squeezing is due to an increase in the strengthening of superconducting grains coupling. Thereafter this increment due to weak coupling among separated superconducting islands increases. These results coincide with the microhardness measurements as well as the data reported elsewhere [28].

4. Conclusions

In the light of the most significant results obtained from different studies, we may say that

1. The given results from the X-ray diffraction and the SEM photographs' studies performed on the considered samples show one to one correspondence, emphasizing that the amount of Pb = 0.3 is most convenient for which maximum amount of high- T_c is formed.
2. An enriching of the Pb content ($x = 0.5$), high- T_c phase (2223) probably dissociates into contaminating phases.
3. Good volumetric arrangement of the superconducting grains has been found to play an important role in the improvement of T_c^0 and the VHN of samples.
4. As a result, an optimum Pb content of $x = 0.3$ for which minimum plus sign of the Seebeck coefficient and maximum T_c^0 are performed.
5. Microhardness of considered samples increases in the Pb content with a corresponding decrease in porosity up to Pb = 0.3, above which the microhardness is decreased and porosity is increased. This increment is due to the formation of contaminating phases such as Ca_2PbO_4 .

References

- [1] H. Maeda, Y. Tanaka, M. Fukutomi, T. Asano, *Jpn J. Appl. Phys.* 27 (1988) L209.
- [2] J.L. Tallon, R.J. Buckley, P.W. Gilberd, R.M. Presland,

I.W.M. Brown, M.E. Bowder, L.A. Dwistian, R. Goguel, *Nature* 333 (1988) 153.

[3] K. Kocabas, *Turkish J. Phys.* 22 (1998) 437–440.

[4] S. Sergeenkova, M. Ausloos, H. Bougrine, R. Cloots, V.V. Gridin, *Phys. Rev. B* 48 (1993) 1680.

[5] M. Sera, S. Tanaka, S. Sato, H. Fujishita, *Solid State Commun.* 81 (1992) 415.

[6] S. Keshri, J.B. Mondal, P. Mondal, A. Poddar, A.N. Das, B. Ghosh, *Phys. Rev. B* 47 (1993) 9048.

[7] S.R. Jha, R. Rajput, D. Kumar, Y.S. Reddy, R.G. Sharma, *Solid State Commun.* 81 (1992) 603–607.

[8] R. Rajput, Y.S. Reddy, R.G. Sharma, G.V. Subbarao, D. Kumar, *Physica C* 213 (1993) 211–218.

[9] M. Pekala, K. Pekala, M.A. Senaris-Rodriguez, F. Garcia-Alvarado, E. Moran, *Solid State Commun.* 77 (1991) 437–439.

[10] G.W. Crabtree, J.W. Downey, B.K. Flandermeyer, J.D. Jorgensen, T.E. Klippert, D.S. Kupperman, W.K. Kwok, D.J. Lam, A.W. Mitchell, A.G. McKale, M.V. Nevitt, L.J. Nowicki, A.P. Paulikas, R.B. Poeppel, S.J. Rothman, J.L. Routbort, J.P. Singh, C.H. Sowers, A. Umezawa, B.W. Veal, J.E. Baker, *Adv. Ceram. Mater.* 2 (1987) 444.

[11] T. Goto, M. Tsujihara, *J. Mater. Sci. Lett.* 7 (1988) 283.

[12] H. Konishi, T. Takamura, H. Kaga, K. Katsuse, *Jpn J. Appl. Phys.* 28 (1989) L241.

[13] M.K. Ihm, B.R. Powell, R.L. Bloink, *J. Mater. Sci.* 25 (1990) 1664.

[14] L.B. Harris, F.K. Nyang, *J. Mater. Sci. Lett.* 7 (1988) 801–803.

[15] H.C. Ling, M.F. Yan, *J. Appl. Phys.* 64 (1988) 1307.

[16] L. Martinez, J.L. Albaran, S. Valdes, J. Fuentes, *Physica C* 152 (1988) 518.

[17] R.E. Loehman, W.F. Hammetter, E.L. Venturini, R.H. Moore, F.P. Gerstle Jr., *J. Am. Ceram. Soc.* 72 (1989) 669.

[18] S.E. Dorris, M.T. Lanagan, D.M. Moffatt, H.J. Leu, C.A. Youngdahl, U. Balachandran, A. Cazzato, D.E. Bloomberg, K.C. Goretta, *Jpn J. Appl. Phys.* 28 (1989) L1415.

[19] H.M. Ledbetter, M.W. Austin, S.A. Kim, M. Lei, *J. Mater. Res.* 2 (1987) 786.

[20] T. Goto, *Jpn J. Appl. Phys.* 28 (1989) L1402.

[21] D.W. Johnson Jr., W.W. Rhodes, *J. Am. Ceram. Soc.* 72 (1989) 2346.

[22] M. Shoyama, H. Nasu, K. Kamiya, *Jpn J. Appl. Phys.* 30 (1991) 950.

[23] S.L. Lubenets, V.D. Natsik, L.S. Fomenko, H.-J. Kaufmann, V.S. Bobrov, A.N. Izotov, *Low Temp. Phys.* 23 (1997) 678–683.

[24] M. Muralidhar, K. Narasimha Reddy, V. Haribabu, *Phys. Stat. Sol. (a)* 126 (1991) 115–120.

[25] C. Veerender, V.R. Dumke, M. Nagabhooshanam, *Phys. Stat. Sol. (a)* 144 (1994) 299.

[26] D. Mangapathi Rao, M. Muralidhar, T. Somaiah, V. Haribabu, *Bull. Mater. Sci.* 14 (2) (1991) 199.

[27] M. Muralidhar, D. Mangapathi Rao, T. Somaiah, V. Haribabu, *Cryst. Res. Technol.* 25 (5) (1990) 561.

[28] D. Mangapathi Rao, T. Somaiah, V. Haribabu, Y.C. Venudhar, *Cryst. Res. Technol.* 28 (1993) 285–298.

[29] W. Herkert, H.W. Neumeller, M. Wilbelem, *Solid State Commun.* 69 (1989) 183.

[30] V. Sima, K. Knizek, J. Chval, E. Pollert, P. Svoboda, P. Vasek, *Physica C* 203 (1992) 59–67.

[31] K. Schulze, P. Majewski, B. Hettich, G. Petzow, *Z. Metallk.* 91 (1990) 836.

[32] M.R. DeGuire, N.P. Bansal, D.E. Farrell, V. Finan, Ch. J. Kim, B.J. Hills, Ch.J. Allen, *Physica C* 179 (1991) 333.

[33] C.J. Kim, C.K. Rhee, H.G. Lee, C.T. Lee, S.J.-L. Kang, D.Y. Won, *Jpn J. Appl. Phys.* 28 (1989) L45–L48.

[34] K.H. Yoon, H.B. Lee, *J. Mater. Sci.* 26 (1991) 5101–5106.

[35] Y.C. Chen, K.K. Chong, T.H. Meen, *Jpn J. Appl. Phys.* 30 (1991) L33.

[36] N. Kijima, H. Endo, J. Tsuchiya, A. Sumiyama, M. Mizano, Y. Oguri, *Jpn J. Appl. Phys.* 27 (1989) L1852.

[37] A. Kikuchi, M. Matsuda, M. Takata, M. Ishii, T. Yamashita, H. Koinuma, *Jpn J. Appl. Phys.* 27 (1988) L2300.

[38] B. Chanda, S.K. Ghatak, T.K. Dey, *Physica C* 232 (1994) 136–144.

[39] L. Forro, L. Lukatela, B. Keszei, *Solid State Commun.* 73 (1990) 501.

[40] C. Uher, A.B. Kaiser, E. Gmelin, L. Walz, *Phys. Rev. B* 36 (1987) 5676.